

Quantitative Imaging and Analysis of SMCC-7721 Cells Using AFAM

Yan Liu, Zuobin Wang, Yujing Zhao

and Xinyue Wang

CNM,

Changchun University of Science and Technology,
Changchun, China;

Yang Yang
College of Mechanical Science and Engineering, Changchun Medical College,
Jilin University, Changchun, China;
*Corresponding author: wangz@cust.edu.cn

Yan Liu

Changchun, China;

Abstract—This paper presents a method for the quantitative imaging and analysis of SMCC-7721 cells using an atomic force acoustic microscope (AFAM). In this work, an AFAM was used to study the surface, intracellular structure and elasticity mapping of SMCC-7721 cells, and both topographic and acoustic images of the cells were obtained. In the experiment, the SMCC-7721 cells were treated with 4% paraformaldehyde (PFA), and untreated and treated with Thymidine (TdR). The imaging results were compared and analyzed. The quantitative analysis result indicates that the AFAM is a useful tool to measure the surface, intracellular structure and the elasticity property of the cells.

Keywords—AFAM; acoustic imaging; SMCC-7721; cell roughness; TdR

I. INTRODUCTION

The atomic force microscope (AFM) has unique advantages in the morphological investigation of material surfaces and structures, and it becomes essential in nano-scale measurement and manipulation in recent years, which has emerged gradually as one of the most potential instruments in cellular, subcellular and molecular mechanics on human diseases including cancers [1-5]. Some examples are in the high-resolution imaging of biomolecules, membranes, organelles and proteins [6-10]. AFM has many modifications for specific applications, and the atomic force acoustic microscope (AFAM) is one of them. The ultrasonic technique, which is commonly used to detect flaws and inhomogeneities inside materials, is combined with the traditional AFM, and can be used to map the surface and subsurface mechanical properties, such as elastic property and hardness. The ultrasonic frequency can be applied to the tip [11] or sample [12], even both the tip and sample can be accomplished [13]. Until now, most AFAMs have been developed to focus on the materials such as nanocrystalline materials [14], thin films [15, 16], polymer composites [17], clay minerals [18], and biomaterials [1, 2, 19, 20].

Cell mechanical properties are useful for understanding pathological processes of diseases [21]. Suresh illustrated that when cytoskeletal architecture induced by drugs changed, the cancer cell mechanics and structure could be influenced [5]. Cross *et al.* found that metastatic cells were softer than normal cells, and suggested that mechanical analysis could distinguish cancerous cells [22]. Plodinec *et al.* applied a force to the cell membrane to obtain stiffness maps and showed that the

mechanical response of cells was a key for disease diagnostics [23]. In this paper, we used an AFAM to image and analyze SMCC-7721 cells. In the experiment, the SMCC-7721 cells were treated with 4% paraformaldehyde, and untreated and treated with Thymidine. By obtaining the topographic and acoustic images of these three groups, the cell surfaces, intracellular structures and mechanical properties were studied. A quantitative comparison of the results indicates that the AFAM is a useful tool to measure the surfaces, intracellular structures and elasticity property of cells, and understand the mechanical properties of cancer cells.

II. METHODS

A. Cell Lines and Reagents

Human hepatocellular carcinoma (SMCC-7721) cell line was used for study. The cells were cultured in the RPMI-1640 medium (Thermo Scientific Hyclone) containing 10% of fetal bovine serum (FBS). They were maintained at 37°C and 5% CO₂ in a humidified incubator. The coverslip (18×18 mm) was placed in the culture dish, by adding a drop of 1.0×10⁶ cells/mL and 2 mL of RPMI-1640 medium with 10% FBS, and incubated for 24 h at 37°C.

B. Sample Preparation

Three petri culture dishes with SMCC-7721 cells were used for experiments, named A, B and C, respectively. After 24 h, 1) Cells in the culture dishes A and C were washed three times with phosphate buffered saline (PBS). 2) And then dish A was fixed with 4% paraformaldehyde (PFA) to immobilize the cells for 15 min, and it was then washed three times with distilled water, and stored at 4°C after soaking up moisture. 3) 1.9 mL 1640 medium with 10% FBS+ 0.1 mL Thymidine (TdR) at the concentration of 100 mM were added to dish C, and continuously incubated for 18 h at 37°C, then removed Thymidine by washing it with PBS three times, and added the fresh 1640 medium with 10% FBS.

C. Atomic Force Acoustic Microscope

An atomic force microscope in ultrasonic mode was set up based on the commercial atomic force microscope (CSPM 5500, Ben Yuan, China). Fig.1 shows the AFAM experimental schematic. The sample was coupled on a piezoelectric transducer that was then bonded to the AFM scanner. A lock-

in-amplifier was used to modulate the amplitude of the cantilever. An AC signal source with the AFM controller was applied to the piezoelectric transducer to drive the sample and the probe being oscillated. The photodiode detected the amplitude and the cell topography, and the lock-in-amplifier and AFM controller then measured the detected signal. By collecting the amplitude and topography data, the subsurface elasticity and topographic images for the sample were reconstructed by computer at the same time.

The probe Tap300Al-G (BudgetSensors, Bulgaria) with the resonant frequency 300 kHz and force constant 40 N/m was used in the experiment. The scanning rate was 1 Hz and the set point force was 0.15 V. The sample imaging was performed in the air.

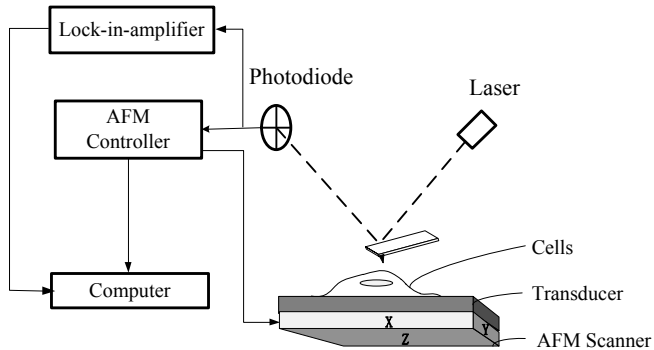


Fig.1. AFAM experimental schematic.

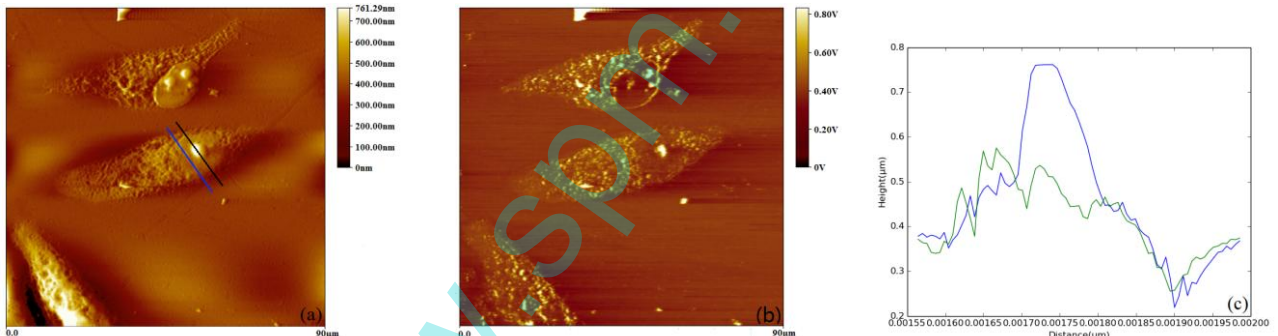


Fig.2. AFAM images of SMCC-7721 cells after immobilizing with 4% PFA. (a) The topography image in $90\mu\text{m} \times 90\mu\text{m}$. (b) The acoustic image in $90\mu\text{m} \times 90\mu\text{m}$. (c) The height curves, in which the blue curve was computed from (a) along the black line and the green curve was computed along the blue line from (a).

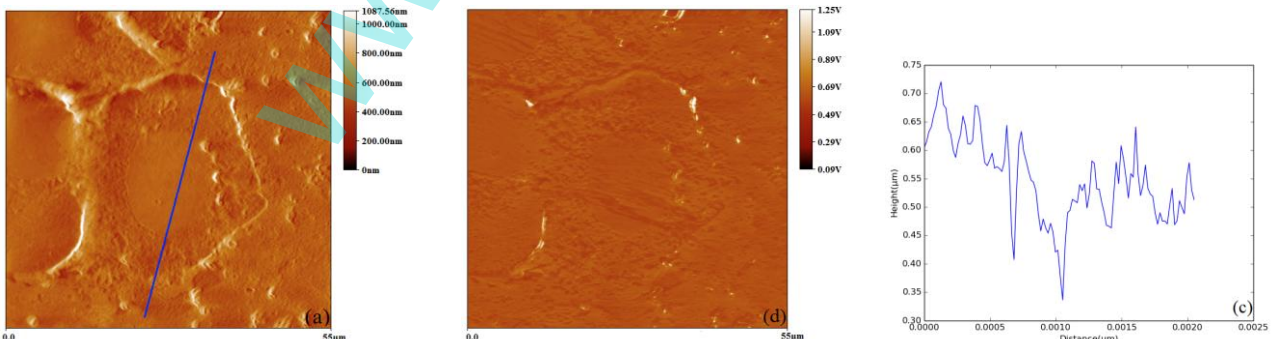


Fig.3. AFAM images of SMCC-7721 cells cultured in the 1640 medium. (a) The topographic images. (b) The acoustic images. (c) The height curve computed from (a) along the blue line.

III. RESULTS AND DISCUSSIONS

We firstly imaged the SMCC-7721 cells immobilized by 4% paraformaldehyde (PFA). The cells were taken from the culture dish A, and we coupled the coverslip with the transducer using Vaseline. Fig.2 shows the AFAM images of the cells after immobilizing with 4% PFA. From the image we can extract the morphological information of the cells, such as the height of each point of the cell surface, and surface roughness [21]. In Fig.2(a), Cytoskeleton has a structure of network and bright thick lines formed by filaments and microtubules, and extends throughout the cytoplasm. The nucleus of the cell seems much higher and smoother than the surrounding areas, as shown in Fig.2(c), but has one or two protuberances on the nucleus of the cells. The protuberances may be nucleolus. In the acoustic images (Fig.2(b)), we can obtain the subsurface mechanical properties of the cells, such as elasticity and stiffness. The brighter areas indicate the stiffer, and the relative darker regions indicate the softer. Compared with the topography image, the edge of nucleus is clearer and the nuclear membrane is shown in Fig.2(b), because of the different elastic properties between the nucleus and the nuclear membrane. Some parts of cytoskeleton could not be seen in Fig.2(a), but they were clearly shown in Fig.2(b).

The cells covered the scaffolds uniformly in the topographic and acoustic images. The topography image indicated the different heights of the cell surface, while more details were shown by the acoustic image due to the heterogeneous structures of cell surface and subsurface. [19]

Fig.3 shows the AFAM images of SMCC-7721 cells that cultured in the 1640 medium and taken from the culture dish B. We first scanned a large area to image many cells and observe the different changes of cell morphology, and then scanned across the interested cells to observe more details. In Fig.3(a), we can see four cells close together, and their nuclei are round or elliptical in shape. The size is increased obviously with the diameter of about 17 μ m, and no protuberances in the center of nucleus. The surfaces of nuclei are smoothly and the nucleolus

is notably found in both topography images and acoustic images. We cannot see the clear structure of cell cytoskeleton in topography image in Fig.3(a). From the acoustic image in Fig.3(b), we can see the thick lines around the cellular outlines that may be the outflow of cytoplasm. The cell cytoskeleton around the nucleus is clearer than that in the topography image. The different results between Fig.2 and Fig.3 may be influenced by the cell status, or the cell lysis, or the outflow of cytoplasm.

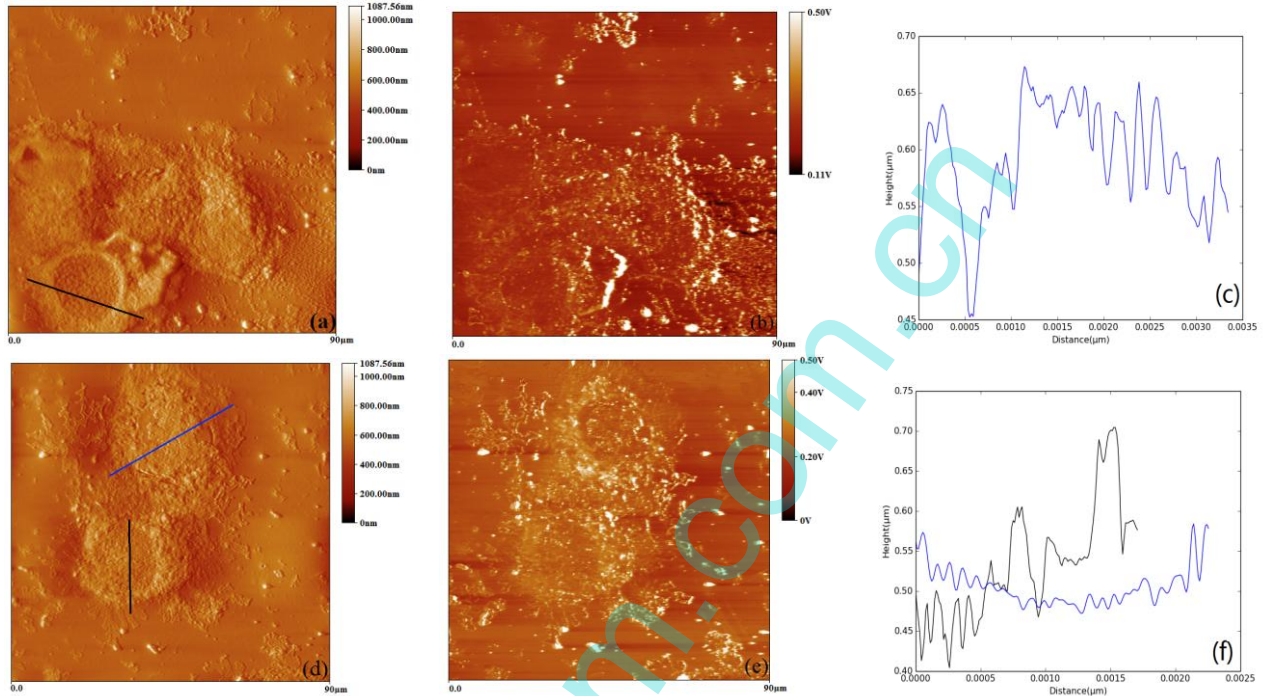


Fig.4. AFAM images of SMCC-7721 cells incubated with the 1640 medium containing 0.1 mL TdR. (a) and (d) were the topographic images. (b) and (e) were the acoustic images. (c) and (f) were the height curves, where (c) was computed from (a), and (f) was computed from (d).

TABLE I. ROUGHNESS VALUES OF SMCC-7721 CELLS

Cell ID	Culture Dish	Roughness (nm)	
		nucleus	cytoplasm
1	A	20.8	52.3
2	A	18.8	43.7
3	B	16.4	40.9
4	B	18.7	36.2
5	C	47.9	52.5
6	C	25.1	52.5
7	C	70.6	76.1

The AFAM images of SMCC-7721 cells taken from dish C and incubated with the 1640 medium containing 0.1 mL TdR

are shown in Fig.4. From the topographic images, cell borders and the edges of nuclei are not recognizable in most cases. We can see only a small number of the cell nuclei in regular circle shapes, e.g. the cell in the bottom-left corner in Fig.4(a). The surfaces of cells are shown with different roughness values. Compared with the topographic images, the results of the acoustic images represented more information that we can observe the outline of the cell nucleus, and many stiff particles of different sizes are found across the subsurface. The different results between Fig.3 and Fig.4 that may be because the cells are under different cell cycles after mixed with TdR, or TdR overdose that can even induce the cell death.

The results in Table I show the surface roughness values of cell nucleus and cytoplasm from three groups. The cell nucleus is smoother than the cytoplasm when the cell after immobilizing with 4% PFA or cultured in the 1640 medium. Whereas, the roughness values of most nucleus are near to cytoplasm, when cultured in the 1640 medium mixed with the 0.1 mL TdR. Comparing the results from the culture dishes B

and C, we can see that the cell roughness is increased on the effect of TdR.

IV. CONCLUSION

In this work, a method for the quantitative imaging and analysis of the topography and subsurface elasticity changes of SMCC-7721 cells was presented. By using the AFAM, both topographic and acoustic images of the cells were obtained. The acoustic images not only recognized the shape but the subsurface elastic mapping. Compared with the topographic images, more details were shown due to the heterogeneous structures of cell surface and subsurface. The quantitative analysis of AFAM images shows that the cells untreated with the immobilization may cause cell collapsed or outflow of cytoplasm, and cells treated with TdR may cause the increase in cell roughness. The result indicates that the AFAM is a useful tool to measure the surfaces, intracellular structures and the elasticity properties of the cells.

Acknowledgment

This work was supported by EU FP7 (BioRA), EU H2020 (FabSurfWAR), International Science and Technology Cooperation Program of China (No.2012DFA11070), and Jilin Provincial Science and Technology Program (Nos.201215136, 20140414009GH, 20140622009JC, 20140414009GH and 20160623002TC).

References

- [1] A. Ebert , B. R. Tittmann , J. Du , and W. Scheuchenzuber, "Technique for rapid in vitro single-cell elastography," *Ultrasound in Medicine & Biology*, vol. 32, pp. 1687–1702, 2006.
- [2] A. M. Ebert , J. Du , X. Wang , and B. Tittmann , "The elastic properties of hamster kidney cells evaluated by ultrasonic atomic force microscopy," *Proceedings of the IEEE Ultrasonics Symposium*, vol.1, pp. 689–692, 2004.
- [3] K. D. Costa, "Single-cell elastography: probing for disease with the atomic force microscope," *Disease Markers*, vol. 19, pp. 139–154, 2004.
- [4] B. S. Elkin, E. U. Azeloglu, K. D. Costa, and B. Morrison, "Mechanical heterogeneity of the rat hippocampus measured by atomic force microscope indentation," *Journal of Neurotrauma*, vol. 24, pp. 812–822, 2007.
- [5] S. Suresh, "Biomechanics and biophysics of cancer cells," *Acta Biomaterialis*, vol. 3, pp. 413–438, 2007.
- [6] J. J. Heinisch, P. N. Lipke, A. Beaussart, S. El-Kirat-Chatel, V. Dupres, D. Alsteens and Y. F. Dufrêne, "Atomic force microscopy-looking at mechanosensors on the cell surface," *Journal of Cell Science*, vol. 125, pp. 4189–4195, 2012.
- [7] Y. F. Dufrêne, "Atomic force microscopy and chemical force microscopy of microbial cells," *Nature Protocol*, vol. 3, pp. 1132–1138, 2008.
- [8] Y. F. Dufrêne, "Towards nanomicrobiology using atomic force microscopy," *Nature Reviews Microbiology*, vol. 6, pp. 674–680, 2008.
- [9] A. Engel, and H. E. Gaub, "Structure and mechanics of membrane proteins," *Annual Review of Biochemistry*, vol. 77, pp. 127–148, 2008.
- [10] D. J. Müller, Y. F. Dufrêne, "Atomic force microscopy: a nanoscopic window on the cell surface," *Trends in Cell Biology*, vol. 21, pp. 461–469, 2011.
- [11] U. Rabe, and W. Arnold, "Acoustic microscopy by atomic force microscopy," *Applied Physics Letters*, vol. 64, pp. 1493–1495, 1994.
- [12] K. Yamanaka, H. Ogiso and O. Kolosov, "Ultrasonic force microscopy for nanometer resolution subsurface imaging," *Applied Physics Letters*, vol. 64, pp. 178–180, 1994.
- [13] G. S. Shekhawat, and V. P. Dravid, "Nanoscale imaging of buried structures via scanning near-field ultrasound holography," *Science*, vol. 310, pp. 89–92, 2010.
- [14] M. Kopycinska-Müller, A. Caron, S. Hirsekorn, U. Rabe, H. Natter, R. Hempelmann, R. Birringer, and W. Arnold, "Quantitative evaluation of elastic properties of nano-crystalline nickel using atomic force acoustic microscopy," *Zeitschrift Für Physikalische Chemie*, vol. 222, pp. 471–498, 2008.
- [15] M. Kopycinska-Müller, R. H. Geiss, J. Müller, and D. C. Hurley, "Elastic-property measurements of ultrathin films using atomic force acoustic microscopy," *Nanotechnology*, vol. 16, pp. 703–709, 2005.
- [16] M. Kopycinska-Müller, A. Clausner, K.-B. Yeap, B. Köhler, N. Kuzeyeva, S. Mahajan, T. Savage, E. Zschech, and K.-J. Wolter, "Mechanical characterization of porous nano-thin films by use of atomic force acoustic microscopy," *Ultramicroscopy*, vol. 162, pp. 82–90, 2015.
- [17] X. L. Zhou, J. Fu, Y. W. Li, and F. X. Li, "Nanomechanical mapping of glass fiber reinforced polymer composites using atomic force acoustic microscopy," *Journal of Applied Polymer Science*, vol. 131, 2014.
- [18] M. Prasad, M. Kopycinska, U. Rabe, and W. Arnold, "Measurement of Young's modulus of clay minerals using atomic force acoustic microscopy," *Geophysical Research Letters*, vol. 29, pp. 13-1–13-4, 2002.
- [19] B. Zhang, Q. Cheng, M. Chen, W. G. Yao, M. L. Qian, and B. Hu, "Image and analyzing the elasticity of vascular smooth muscle cells by atomic force acoustic microscope," *Ultrasound in Medicine & Biology*, vol. 38, pp. 1383–1390, 2012.
- [20] S. Zhang, H. Aslan, F. Besenbacher, and M. D. Dong, "Quantitative biomolecular imaging by dynamic nanomechanical mapping," *Chemical Society Reviews*, vol. 43, pp. 7412–7429, 2014.
- [21] M. Li, L. Q. Liu, N. Xi, Y. C. Wang, X. B. Xiao, and W. J. Zhang, "Quantitative analysis of drug-induced complement-mediated cytotoxic effect on single tumor cells using atomic force microscopy and fluorescence microscopy," *IEEE Transactions on Nanobioscience*, vol. 14, pp. 84–94, 2015.
- [22] S. E. Cross, Y. S. Jin, J. Rao, J. K. Gimzewski, "Nanomechanical analysis of cells from cancer patients," *Nature Nanotechnology*, vol. 2, pp. 780–783, 2007.
- [23] M. Plodinec, M. Loparic, C. A. Monnier, E. C. Obermann, R. Zanetti-Dallenbach, P. Oertle, J.T. Hyotyla, U. Aebi, M. Bentires-Alj, C.A. Schoenenberger, "The nanomechanical signature of breast cancer," *Nature Nanotechnology*, vol. 7, pp. 757–765, 2012.